Heliyon 6 (2020) e03266

Contents lists available at ScienceDirect

Heliyon

journal homepage: www.cell.com/heliyon

Research article

Nanofibrils *vs* nanocrystals bio-nanocomposites based on sodium alginate matrix: An improved-performance study

B. Deepa [a], E. Abraham [b], N. Cordeiro [c,d,**], M. Faria [c], G. Primc [e], Y. Pottathara [f], M. Leskovšek [g], M. Gorjanc [g], M. Mozetič [e], S. Thomas [h], L.A. Pothan [a,*]

[a] Department of Chemistry, C.M.S.College, Kottayam, 686001, Kerala, India
[b] Renewable and Sustainable Energy Institute, University of Colorado, Boulder, Colorado, 80309, USA
[c] LB3, Competence Centre in Exact Science and Engineering, University of Madeira, 9000-390, Funchal, Portugal
[d] CIIMAR-Interdisciplinary Centre of Marine and Environmental Research, University of Porto, 4450-208, Matosinhos, Portugal
[e] Department of Surface Engineering and Optoelectronics, Jozef Stefan Institute, Jamova cesta 39, 1000, Ljubljana, Slovenia
[f] University of Maribor, Faculty of Mechanical Engineering, 2000, Maribor, Slovenia
[g] Faculty of Natural Sciences and Engineering, University of Ljubljana, Aškerčeva 12, 1000, Ljubljana, Slovenia
[h] International and Inter University Centre for Nanoscience and Nanotechnology, Mahatma Gandhi University, Kottayam, 686560, Kerala, India

ARTICLE INFO

Keywords:
Materials science
Nanotechnology
Nanomaterials
Materials characterization
Materials property
Agricultural technology
Nanofibrils
Nanocrystals
TEMPO-Mediated oxidation
Sodium alginate
Kapok fiber
Nanocomposite

ABSTRACT

To develop bio-nanocomposites using natural biopolymers, nanocomposite films were prepared based on sodium alginate and kapok nanofibrils (CNFs). CNFs when subjected to TEMPO-mediated oxidation gave rise to cellulose nanocrystals (TOCNCs), with carboxyl groups at the surface (K_a/K_b = 3.64). The differences between the two types of nanocelluloses (nanofibrils and nanocrystals) and their impact in the preparation of bio-nanocomposites, were studied. When incorporated in the matrix, the CNFs particles have the tendency to form surface aggregation (K_a/K_b = 2.37), distorting the alginate network, creating heterogeneous films, with high surface roughness (S_a = 29.37 nm), porosity (D_p = 0.087 cm^2/min) and vulnerability to heat. The TOCNCs present good dispersion creating a 3D network, which forms uniform (D_p = 0.122 cm^2/min) and homogeneous films, with smooth surface (S_a = 16.83 nm). The ultrasonication treatment facilitated the dispersion improving the interfacial interaction between the reinforcing phase and the matrix. The results show the reinforcement potential of kapok nanocellulose in an industrially and medically important biopolymer, sodium alginate, especially when TOCNCs and ultrasonication were used.

1. Introduction

Bio-nanocomposites made from polymeric matrix and nanoscale-reinforcing agents have received growing attention due to the increasing environmental consciousness and demand for green and biocompatible products. Varieties of natural polymers have been used to produce bio-nanocomposites, among which, natural biopolymers such as sodium alginate and cellulose have attracted a great deal of interest due to their characteristic features like biodegradability, biocompatibility, low-toxicity, colloidal stability, easiness of process and eco-friendly nature. Alginate has been widely used as an excellent biomaterial in many fields such as tissue engineering, drug delivery, food packaging and biomedical applications. However, the poor mechanical strength and uncontrolled degradation properties pose a drawback for their extensive usage.

The kapok is a gigantic tree of the tropical forest canopy and emergent layer. The seed-hair fiber obtained from the fruit of the kapok tree is an underutilized natural fiber material, spread cross Central America and the Caribbean, west Africa and southern Asia. Being a highly rich source of cellulose makes it very attractive for industrial applications due to the inexpensive components production of environmentally friendly materials.

Cellulose is one of the most abundant natural biopolymers produced in the biosphere and is composed of β-1-4-linked D-anhydroglucose units. It serves as a virtually inexhaustive source of raw material with a wide range of applications. This is due to its inherent characteristics such as

* Corresponding author.
** Corresponding author.
E-mail addresses: ncordeiro@staff.uma.pt (N. Cordeiro), lalybmc@gmail.com (L.A. Pothan).

https://doi.org/10.1016/j.heliyon.2020.e03266
Received 22 May 2019; Received in revised form 1 December 2019; Accepted 16 January 2020

low cost, low density, renewability, abundant availability, biodegradability, high specific mechanical strength and surface modification easiness (Moon et al., 2011). Recently, nanocellulose has been proclaimed as a versatile green nanomaterial due to its unique features such as nanoscale dimension, large specific surface area, high aspect ratio, high strength and stiffness, biocompatibility, biodegradability, low cost, low density and low thermal coefficient of expansion (Abraham et al., 2011; Deepa et al., 2011; Moon et al., 2011). Several studies reported nanocellulose to be a reinforcement filler in alginate matrix. It has different applications such as coated sutures on various tissues and regenerative medicine (Laurén et al., 2017), used for immobilization of lipase (Kim et al., 2017), food packaging material (Sirviö et al., 2014), micro encapsulation of probiotic (Huq et al., 2012) and adsorption of trace metals (Hu et al., 2018). Studies revealed that the tensile strength, elastic moduli, optical transparency and thermal stability of developed bio-nanocomposite films increased with the addition of nanocellulose.

The presence of active hydroxyl groups on the nanocellulose surface provides reactive platforms for chemical modifications, including esterification, oxidation, and polymer grafting (Habibi et al., 2006; Moon et al., 2011; Qin et al., 2015). These surface modification methods facilitate an effective incorporation of nanocellulose within non-polar or hydrophobic polymer matrices. Among these methods, TEMPO (2,2,6,6-tetramethylpiperidine-1-oxyl)-mediated oxidation can oxidize hydroxyl groups to their corresponding carboxylic form (Habibi et al., 2006; Isogai et al., 2011). It has been widely reported that the incorporation of TEMPO-mediated oxidized nanocellulose into biopolymer can result in the preparation of bio-nanocomposites with improved mechanical, optical, thermal and barrier properties (Cheng et al., 2017; Hassan et al., 2018). In a recent study by Hassan et al. (2018), similar improvements in mechanical, thermomechanical and moisture barrier properties of hydroxypropyl methylcellulose bioactive films prepared by the incorporation of TEMPO-mediated oxidized nanocellulose have been reported. These results are encouraging and therefore it is of great interest to investigate the outstanding nano-reinforcement effect of TEMPO-oxidized nanocellulose in biopolymeric matrices.

In view of the valorization of the kapok tree fruit, and due to their attractive surface and morphologic properties (Deepa et al., 2015), nanocomposite films based on sodium alginate and nanofibrils (CNFs) obtained from kapok cellulose suspension were prepared by the solution casting technique. To prepare improved-performance bio--nanocomposites, CNFs were subjected to TEMPO-mediated oxidation. The differences between the two types of nanocelluloses obtained, were studied in terms of the surface properties. However, the principal focus of the present work was the investigation of the effect of these nanocellulose on the structural, morphological, visco-elastic and, mainly, surface characteristics of the prepared nanocomposite films, by various characterization techniques such as X-ray diffraction (XRD), scanning electron microscopy (SEM), atomic force microscopy (AFM), dynamic mechanical analysis (DMA) and inverse gas chromatography (IGC).

It is known that nanocellulose materials are highly segregated in aqueous environment. Thus, the ultrasonication, an efficient method reported in the literature (Zhou et al., 2018; Shen et al., 2017, Qin et al., 2015) to disperse materials in a solution, was also studied in order to obtain bio-nanocomposites able to be applied as tissue engineering scaffolds.

2. Experimental

2.1. Materials

CNFs were extracted from the fruit of kapok tree from Kollam district, Kerala, India. The chemicals used for the extraction of CNFs were sodium hydroxide (NaOH), sodium chlorite ($NaClO_2$), acetic acid (CH_3COOH) and oxalic acid ($H_2C_2O_4.2H_2O$) of laboratory grade purchased from Merck (Mumbai, India). The reagents used for the TEMPO-mediated oxidation process of CNFs include 2,2,6,6-tetramethyl-piperidinyl-1-oxyl (TEMPO), sodium bromide (NaBr), sodium hypochlorite (NaClO) and ethanol. These were purchased from Sigma-Aldrich. The sodium alginate (sodium salt of alginic acid obtained from brown algae) was supplied by Loba Chemie (Mumbai, India) and the glycerol (99.5%) was purchased from Merck (Mumbai, India).

2.2. Extraction of CNFs and TEMPO-mediated oxidation

CNFs was extracted from kapok fibers using the methodology reported by Deepa et al. (2015). Briefly, the fibers were subjected to three distinct treatments: *(i)* alkaline treatment, *(ii)* bleaching and *(iii)* acid hydrolysis. Initially, the fibers were subjected to steam explosion with 2% NaOH in an autoclave (20 lbs at 110–120 °C) and after that washed in distilled water until neutral pH. Then, the insoluble residue was bleached with an acidified sodium chlorite solution at 70 °C for 1 h, neutralized with NaOH solution, washed with distilled water and dried in a vacuum oven at 60 °C. The bleached cellulose pulp was then hydrolyzed with 5% oxalic acid solution for 3 h in an autoclave (20 lbs). After that, fibers were taken out, filtered and rinsed with distilled water until neutral pH. In order to obtain a homogeneous suspension of CNFs, the pulp solution was mechanically stirred for 6 h.

TEMPO-mediated oxidation was carried out using TEMPO (2,2,6,6-tetramethylpiperidine-1-oxyl) free radical reagent, sodium bromide and sodium hypochlorite (NaClO) according to the procedure described by Isogai et al. (2011), Saito et al. (2007) and Yasir Beeran et al. (2016). Briefly, sodium bromide and TEMPO (10 wt%) were added dropwise into the CNFs suspension (2 wt%). The TEMPO-mediated oxidation reaction was started by the addition of a desired amount of NaClO (12 wt%) solution to the suspension and adjusting the pH to 10. The mixture was stirred for 3 h at room temperature. The reaction was quenched by the addition of ethanol, and then the pH was adjusted to 7. The final suspension was thoroughly washed and stored at 4 °C before further treatment or analysis. The obtained fibers were named as TOCNCs. Figure 1 shows the schematic diagram of TEMPO-mediated oxidation of nanocellulose.

2.3. Preparation of alginate and bio-nanocomposite films

Pure alginate and bio-nanocomposite films based on sodium alginate (SA) and nanocellulose (CNFs and TOCNCs) were prepared via solution casting technique described by Deepa et al. (2016). Ultrasonication of nanocellulose suspension (US) were carried out using a low frequency ultrasound at 20 KHz with a power of 500 W and 50% amplitude, in order to obtain a uniform dispersion of nanocellulose in alginate matrix. Nanocomposite films were prepared by the incorporation of 10 wt% of nanocellulose suspension into the alginate matrix with ultrasonication (named as 10% US CNFs/SA and 10% US TOCNCs/SA) and without ultrasonication (named as 10% CNFs/SA and 10% TOCNCs/SA). Nanocellulose suspension was slowly added to the solution of sodium alginate and the resulting mixture was stirred at 60–70 °C for 1 h. The obtained film forming solution was transferred into a petri dish with 14 cm in diameter and dried in an oven at 40 °C for two days. The obtained dried films were kept in polyethylene covers prior to further characterization. The obtained nanocomposites were named regarding the applied treatment.

2.4. Characterization methods

2.4.1. Atomic force microscopy (AFM)

AFM measurements were performed in a Shimadzu SPM-9600 equipment to evaluate the thickness of the nanocellulose particles. A drop of diluted aqueous suspension was deposited onto a freshly cleaved mica surface and air-dried. AFM images were obtained at room temperature in the dynamic mode with a scan rate of 1 Hz, using Si tips with a curvature radius of less than 10 nm and a spring constant of 42 Nm^{-1}.

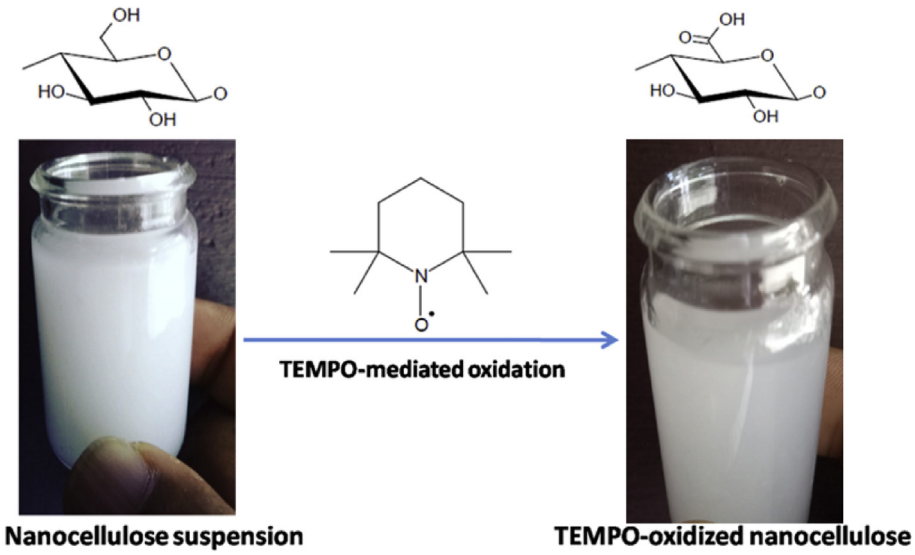

Figure 1. TEMPO (2,2,6,6-tetramethylpiperidine-1-oxyl)-mediated oxidation of nanocellulose.

Surface morphology of the prepared films was also analyzed by atomic force microscopy (AFM, Solver PRO, NT-MDT, Russia) in tapping mode in air. Samples were scanned with the standard Si cantilever with a force constant of 22 N m^{-1} and at a resonance frequency of 325 kHz (tip radius was 10 nm and the tip length were 95 μm). Average surface roughness (S_a) was measured from representative images on 5 × 5 μm^2 areas and the scan rate was set at 1.3 Hz.

2.4.2. ^{13}C-cross polarization magic angle spinning nuclear magnetic resonance (^{13}C-CPMAS NMR) spectroscopy

^{13}C-CPMAS NMR spectra were recorded on a Bruker Avance III 400 spectrometer operating at a B_0 field of 9.4 T using 9 kHz MAS with proton 90° pulse of 3 μs and a time between scans of 3 s. ^{13}C-CPMAS NMR spectra were acquired using a contact time of 2000 μs. ^{13}C chemical shifts were referenced with respect to glycine (C=O at 176.03 ppm).

2.4.3. Inverse gas chromatography (IGC)

Surface characteristics of samples were investigated using a commercial inverse gas chromatograph (SMS-*i*GC, 2000; London, UK). The IGC measurements were conducted according to the work reported by Cordeiro et al. (2011). *n*-Alkane series (C_6 to C_{10}) were used to measure the dispersive component of surface free energy (γ_s^d). Acetonitrile (ACN), ethyl acetate (EtOAc), ethanol (EtOH), acetone (AC) and tetrahydrofuran (THF) were used for the determination of the acid-base surface character (K_a and K_b). *n*-octane was used to measure the degree of permeability (D_p). All the measurements were performed at 20 °C.

2.4.4. X-ray diffraction (XRD)

XRD analysis of the films were conducted using an X-ray diffractometer (Bruker AXS D8 Advance, Germany), equipped with Cu Kα radiation source (wavelength 0.154 nm) operating at 40 kV and 30 mA. The XRD patterns were recorded over the angular range $2\theta = 0$–50° with a step interval of 0.02°.

2.4.5. Scanning electron microscopy (SEM)

Morphological studies of the films were performed using a Jeol JSM-7600F (USA) Schottky Field Emission Scanning Electron Microscope. It is a semi in-lens SEM with high resolution. The samples were coated with a layer of gold about 30 nm thick. For SEM imaging, LEI (below-the-lens secondary electron detector) mode was used. In order to see the actual surface, LEI mode was used with the accelerating voltage of 5 kV at the working distance of 15 mm.

2.4.6. Dynamic mechanical analysis (DMA)

Measurements of mechanical properties of the films were performed on a dynamic mechanical analyzer Q800 DMA (TA Instruments, USA) with a controlled gas cooling accessory (GCA). Multi-Frequency-Strain measurements were performed in film tension mode of deformation with the length of 12 mm and width of 0.7 mm of the samples. Measurements were performed at temperature range of 0–250 °C, heating rate of 3 °C min^{-1}, amplitude of deformation 10 μm and frequency of deformation 10 Hz. The following data were obtained from the results of measurements: glass transition temperatures (T_g), elastic (storage) modulus E′, loss modulus E″ and damping factor (tan δ) as function of temperature (T).

3. Results and discussions

3.1. TEMPO-mediated oxidation

The extracted CNFs were subjected to a TEMPO-mediated oxidation modification in order to obtain nanocellulose with improved-performance properties. AFM images were taken to examine the changes of the morphology and dimension of nanofibrils, before and after the TEMPO-mediated oxidation process. CNFs exhibited a typical rod-like morphology with an average length of 519 ± 167 nm (Figure 2A) and an average width of 4.72 ± 2.29 nm. After the TEMPO-mediated oxidation, the average length of nanocellulose decreased to 381 ± 116 nm and the average width slightly decreased to 3.55 ± 1.37 nm (Figure 2B). These results indicate that the TEMPO-mediated oxidation process of CNFs promotes the disintegration of CNFs into smaller particles, cellulose nanocrystals (CNCs). The XRD data of CNFs and TEMPO-oxidized CNFs (Figure 2C) show a significant increase in the crystallographic plane characteristics of the crystalline region, which corroborates the conclusion made. Saito et al. (2007) reported that mechanical disintegration in an aqueous solution makes the fibers slightly shorter and with a rod-like morphology.

The ^{13}C-CPMAS NMR spectra of CNFs before and after TEMPO-mediated oxidation are presented in Figure 3. The NMR spectrum of CNFs has six signals, one for each C atom. The peaks that have chemical shift values at 105.2 ppm and 88.9 ppm are assigned to C1 and C4, respectively (Saito et al., 2005; Sharma et al., 2017). The peaks from 84.3 ppm to 74.9 ppm correspond to C2, C3 and C5 and are not easily separated due to overlapping (Lai et al., 2013; Saito et al., 2005). The peak at 62.7 ppm corresponds to C6 primary hydroxyl groups exposed to the

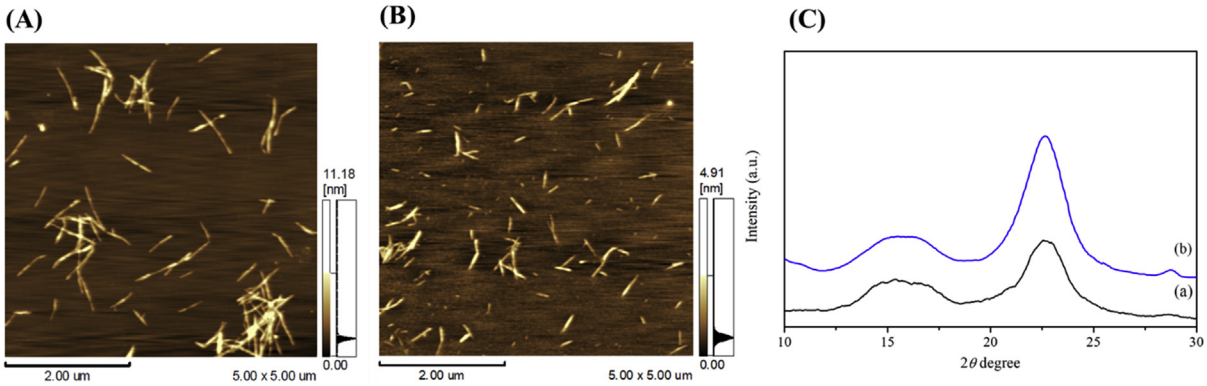

Figure 2. AFM images of CNFs before (A) and after TEMPO-mediated oxidation (B) and, X-ray diffraction patterns (C) of CNFs before (a) and after (b) TEMPO-mediated oxidation.

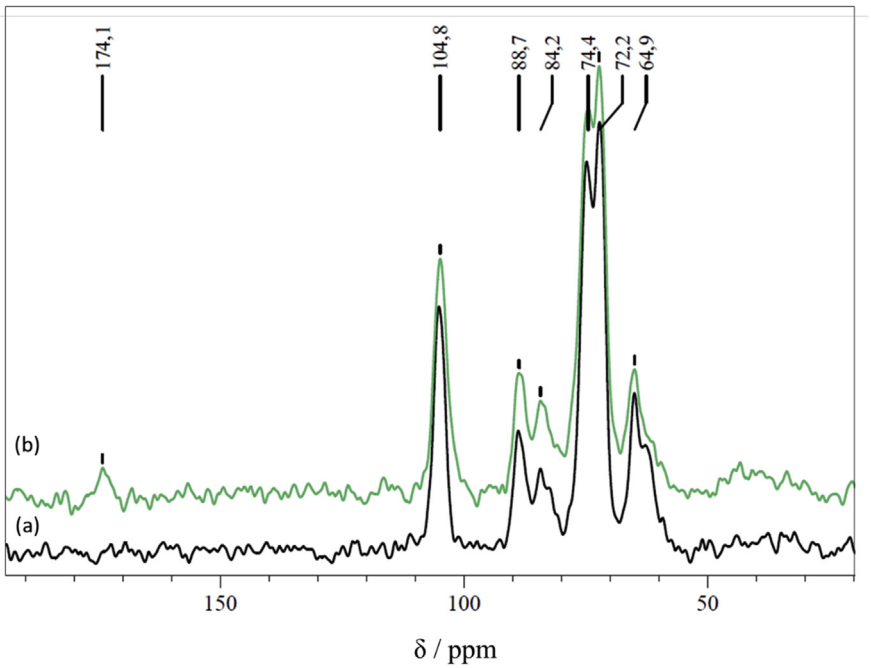

Figure 3. ^{13}C-CPMAS NMR spectra of CNFs before **(a)** and after **(b)** TEMPO-mediated oxidation.

CNFs surface (Viëtor et al., 2002). The carbon signal at 64.8 ppm corresponds to the C6 primary hydroxyl groups inside the crystalline CNFs and to C2/C3 ratio, which remains unchanged (Lai et al., 2013). TEMPO-oxidation of the hydroxyl groups of CNFs leads to some visible changes on the NMR spectrum of the modified nanocellulose. The most prominent changes are the appearance of the carboxylate carbon peaks at 174 ppm and the disappearance of the peak at 62.7 ppm, which corresponds to C6 primary surface hydroxyl groups (Lai et al., 2013; Saito et al., 2005). The other carbon peaks of the oxidized sample are observed at 104.6 ppm (C1), 88.2 ppm (C4), 83.8–72.2 ppm (C2, C3 and C5) and 64.8 ppm (interior C6 primary –OH groups), which are analogous to the CNFs profile. These results provide evidence for the success of TEMPO-oxidation for the modification of C6 primary hydroxyl group to carboxyl group in cellulose chains.

To confirm the referred changes in the nanocellulose at the molecular level, the acid/base characteristics of the surface were studied by inverse gas chromatography (IGC). An increase in K_a and a decrease in K_b (Table 1) were observed after TEMPO-oxidation process. This is a confirmation of the TEMPO-oxidation of the C6 primary hydroxyl groups to carboxyl groups present at the surface of cellulose. It can be concluded from the above results that the TEMPO-mediated oxidation of CNFs allows the formation of oxidized CNCs particles with carboxyl groups at the surface (named as TOCNCs).

3.2. Characterization of bio-nanocomposites

The ultrasonication has been reported as an efficient method to disperse materials in a solution. Knowing that nanocellulose materials are highly segregated in aqueous environment, the benefits of

Table 1. Surface energy of nanocelluloses before (CNFs) and after (TOCNCs) TEMPO-mediated oxidation at 20 °C.

Nanocellulose	γ_s^d (mJ/m^2)	K_a	K_b	K_a/K_b
CNFs	36.74	0.088	0.032	2.75
TOCNCs	37.61	0.091	0.025	3.64

γ_s^d: dispersive component of surface free energy; K_a: dissociation constant of acid; K_b: dissociation constant of base.

ultrasonification for the newly produces renewable bio-nanocomposites were studied.

XRD analysis was carried out to understand the effect of ultrasonication (US) and TEMPO-oxidation (TOCNCs) treatments on the crystalline structure and orientation of nanocellulose within alginate matrix. Figure 4 depicts the XRD patterns of pure alginate films (SA) and nanocomposite films. The XRD pattern of SA did not show any distinct crystalline characteristic peaks, which would reveal the amorphous structure of alginate (Figure 4a). However, the XRD pattern of the nanocomposites revealed a crystalline nature with the incorporation of nanocellulose into the alginate matrix. The diffraction peaks observed at around 14.8° and 22.5° can be attributed to the (11 0) and (200) crystallographic planes of cellulose I structure (Cheng et al., 2017). Differences can be observed in the XRD pattern for the different nanocomposite films prepared with the CNFs and TOCNCs, with and without ultrasonication process (Figure 4b-e). The nanocomposite films prepared with CNFs and without the ultrasonication process (Figure 4b) exhibited broad peaks with minimum intensity. These diffraction peaks become more prominent in the XRD pattern of film samples prepared with TEMPO-oxidized cellulose nanocrystals (Figure 4b *vs* 4d or Figure 4c *vs* 4e) and with the ultrasonication treatments (Figure 4b *vs* 4c or Figure 4d *vs* 4e). Besides that, the addition of TOCNCs provokes a more pronounced effect than with ultrasonication dispersion. Within all the nanocomposites the most prominent cellulose diffraction peaks is obtained in the case of ultrasonicated TOCNCs films (Figure 4b-e). This may be due to the presence of a more homogenous dispersion and partially oriented nanocrystal particles within the nanocomposite films. Due to the TOCNCs structural and chemical nature, the ultrasonication allows their dispersion and establishment of new interactions, leading to reorganization, and orientation of the nanocrystal particles. This result is consistent with the study of the crystalline properties of sodium alginate-xanthan gum-based nanocomposite scaffolds reinforced with CNCs (Kumar et al., 2017) or with the bio-nanocomposite films based on pectin and CNCs reported by Chaichi et al. (2017).

The morphological examination of the samples under study using SEM analysis was performed to evaluate the effect of CNFs and TOCNCs and ultrasonication process on the microstructure and homogeneity of the prepared nanocomposite films. Figure 5 presents the surface microstructure images of pure alginate and nanocellulose reinforced alginate films.

As shown in Figure 5, pure alginate (SA) has a smooth surface compared to the nanocomposite films. The surface of the nanocomposite films with the nanofibrils incorporation was found to be rougher than the neat alginate film as well as the film with the incorporation of oxidized nanocrystals. This indicates that the CNFs particles within the alginate matrix have higher tendency for agglomeration than the TOCNCs. Additionally, the ultrasonicated TOCNCs particles are more homogeneously dispersed in the alginate matrix since the surface roughness of the sample decreased. Based in Abdollahi et al. (2013) and Qin et al. (2015) this may be due to the lower tendency for agglomeration of the TOCNCs and the higher hydrogen bonding capacity, which could promote strong interfacial interactions between the filler and the matrix.

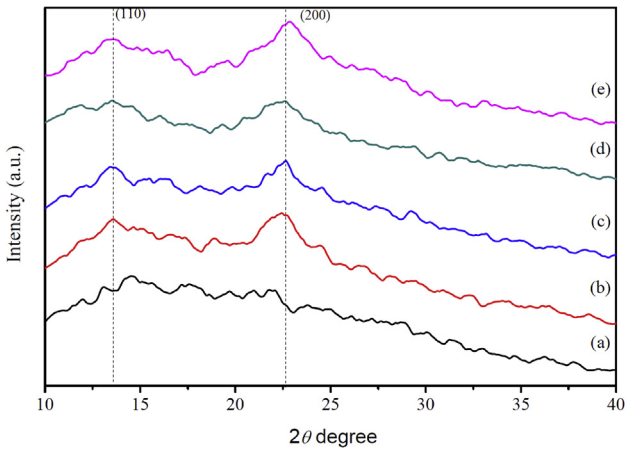

Figure 4. XRD patterns for SA film (a)and for 10% CNFs/SA (b), 10% US CNFs/SA (c), 10% TOCNC/SA (d), 10% US TOCNCs/SA (e)nanocomposites.

Atomic force microscopy (AFM) analysis was also performed to confirm the reduction in surface roughness values of the nanocomposites after the TEMPO-mediated oxidation and ultrasonication process. Figure 6 presents 3D and 2D tapping mode AFM images of the pure alginate and nanocomposite films and the values of average surface roughness (S_a). It is clear from the AFM images that both treatments (TEMPO-oxidation and ultrasonication) have a significant effect on the surface morphology of the nanocomposite films. Pure alginate film displays a smooth surface with an average S_a value of 5.49 nm (Figure 6a). CNFs/SA film (Figure 6b) exhibited a rough surface texture with the highest average value of S_a (29.37 nm), whereas the films with TOCNCs and ultrasonication (Figure 6e) showed the lowest average value of surface roughness (8.52 nm). Bio-nanocomposite films prepared with CNFs and ultrasonication process (Figure 6c) displayed S_a value of 21.26 nm and those prepared only with TOCNCs (Figure 6d), exhibited S_a value of 11.86 nm, which are higher than that of the films prepared using both treatments combined.

As the minimum value of surface roughness is an indication of good dispersion of particles in the matrix, it can be concluded from these results that both ultrasonication and TEMPO-oxidation treatments can enhance dispersion of nanocellulose particles in the alginate matrix with less aggregation of the particles and thereby improving the interfacial interaction between the reinforcing phase (nanocellulose) and matrix phase (alginate).

The surface properties of CNFs and TOCNCs reinforced alginate films were studied by IGC analysis. The determined surface physico-chemical parameters are presented in Table 2. There is only a slight difference in the dispersive component of the surface energy (values of all film samples). This may be due to the similar polysaccharide structure of the biopolymers. However, the interaction between bio-nanocomposites surface groups and IGC polar probes presents significant differences relatively to the pure alginate film. The K_a/K_b ratio of CNFs incorporated alginate film is quite high (2.37), near the value of K_a/K_b ratio of the CNFs (2.75). This is due to the presence of the CNFs at the nanocomposites surface, explaining the high surface roughness (29.37 nm) of this film sample, detected by the AFM. When the addition of CNFs was followed by the ultrasonication process, an increase of the surface basicity was observed, indicating that the CNFs are inside the alginate matrix. The CNFs incorporation in the alginate matrix gives rise to a structural rearrangement and a surface orientation of the glucose moieties basic groups (C–O–C). From Table 2, it can also be observed that 10% US TONCs/SA film sample has the same K_a/K_b ratio (1.9) as the pure alginate film. This means that smaller particle size of TOCNCs and the good dispersion of TOCNCs in alginate matrix by ultrasonication resulted in a more homogeneous film, explaining the smooth surface observed by AFM (surface roughness of 8.52 nm). These results confirm that ultrasonication treatments are required to provide uniform dispersion and better interaction between the TOCNCs and the alginate matrix, in order to obtain a homogeneous film surface without altering the acid-base properties.

The degree of permeability (D_p) gives an indication about the porosity/compaction of the film: more porous or less compact the film, higher is the D_p. Consequently, the highest value of D_p (Table 2) for 10% CNFs/SA and 10% US CNFs/SA films indicates distortion of the alginate network, creating more pores in the matrix. This confirms the CNCs aggregation and the formation of heterogeneous bio-nanocomposites. Pure alginate and 10% US TOCNCs/SA films have similar values for D_p, confirming that the addition of nanocrystals followed by ultrasonication gives rise to homogeneous films.

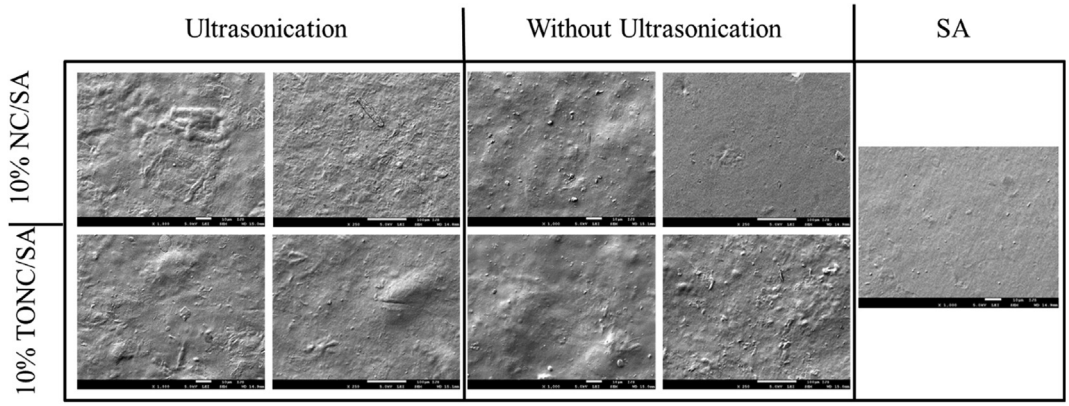

Figure 5. SEM images of SA film and nanocomposites obtained with 10% CNFs and 10% TOCNCs, with and without ultrasonication process.

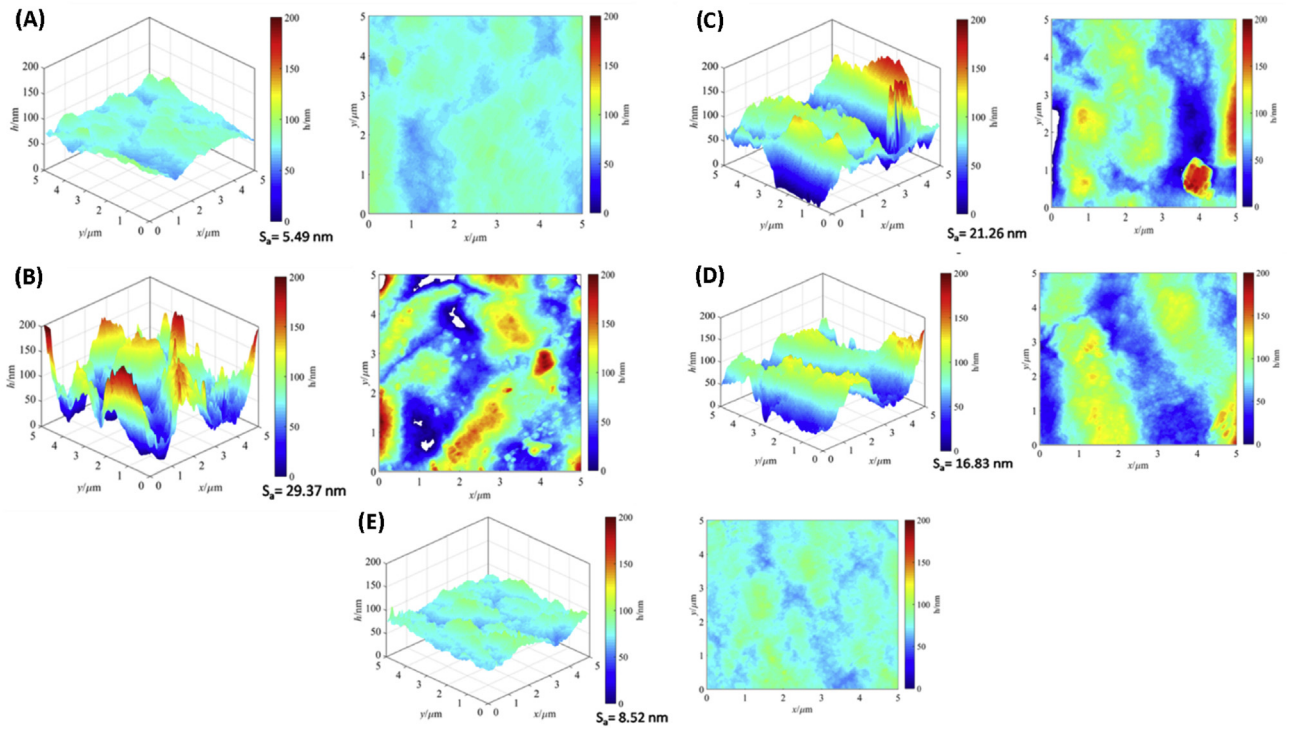

Figure 6. AFM 3D images and 2D surface topography for SA film (A)and for 10% CNFs/SA (B), 10% US CNFs/SA (C), 10% TOCNCs/SA (D)and 10% US TOCNCs/SA (E) nanocomposites.

D_p gives an indication about the porosity of the film (Table 2): more porous or less compact the film, the higher is the D_p. Thus, the highest value of D_p for 10% CNF/SA and 10% US CNFs/SA films indicates distortion of the alginate network, creating more pores in the matrix. This confirms the CNFs aggregation and the formation of heterogeneous nanocomposite film surface. Pure alginate and 10% US TOCNCs/SA samples have the lowest values of D_p, indicating that the addition of TOCNCs followed by ultrasonication lead to homogeneous film surface. It can be concluded from these results that the TEMPO-oxidation and ultrasonication treatments have a significant impact on altering the surface physico-chemical properties of the nanocomposite films.

Table 2. Surface properties of pure alginate film and bio-nanocomposites under study at 20 °C by IGC.

Sample	γ_s^d (mJ/m^2)	K_a	K_b	K_a/K_b	Dp (cm^2/min)
SA	34.10	0.083	0.044	1.89	0.087
10% CNFs/SA	33.90	0.083	0.035	2.37	0.142
10% TOCNCs/SA	33.61	0.082	0.059	1.39	0.122
10% US CNFs/SA	33.78	0.085	0.059	1.27	0.151
10% US TOCNCs/SA	35.68	0.083	0.043	1.93	0.090

γ_s^d: dispersive component of surface free energy; K_a: dissociation constant of acid; K_b: dissociation constant of base; Dp: degree of permeability.

RoyChowdhury and Kumar (2006) showed that porous oxidized cellulose membranes were able to support cells adhesion and proliferation; hence, the obtained bio-nanocomposites exhibit potential to be used as tissue engineering scaffolds.

DMA was used to determine the temperatures of glassy and other relaxation transitions (T_g and T_t), elastic modulus (or storage modulus, E'), viscous modulus (or loss modulus, E'') and damping coefficient (tan δ). The temperatures of transition of the film samples under study were determined from the curves of storage modulus E' and both parameters are provided in Table 3. The viscoelastic curves are presented as graphical plots of E', E'', and tan δ versus temperature in Figure 7.

Table 3. DMA data obtained for alginate and bio-nanocomposites under study at 20 °C.

Sample	T_g (°C)	T_t (°C)	E' (GPa)
SA	21.26	166.71	1.980
10% CNFs/SA	26.42	159.14	2.531
10% TOCNCs/SA	33.49	150.03	4.348
10% US CNFs/SA	17.03	154.83	3.958
10% US TOCNCs/SA	25.88	156.99	4.499

T_g: glass transition temperature; T_t: transition temperature; E': storage modulus.

The viscoelastic curves of all samples mainly show two temperature relaxation transition regions: 0–50 °C and 70–200 °C. The first relaxation region belongs to the glass transition (T_g) of the samples. The pure alginate has a transition point at 21.26 °C, as shown in Table 3. The transition points of all composites are higher than in pure alginate, except for 10% US CNFs/SA where T_g drops to 17.03 °C. The 10% TOCNCs/SA shows the highest thermal stability of viscoelasticity ($T_g = 33.49$ °C). The dispersion of CNCs into the alginate matrix is less homogenous in the absence of ultrasonication. The ultrasonicated TEMPO-oxidized sample (10% US TOCNCs/SA) exhibits higher transition temperature (25.88 °C) than the pure alginate. This suggests that TOCNCs interact with the alginate component forming a cross-linked complex in which TOCNCs are more homogeneously dispersed (due to the ultrasonication). The complex structure is less prone to the thermal chain mobility, which raises T_g. The 10% CNFs/SA shows less reactivity and might be less homogeneously dispersed in alginate matrix. That hinders the mobility of alginate chains and therefore again raises T_g of this sample ($T_g = 26.42$ °C). As mentioned earlier, 10% US CNFs/SA shows the lowest T_g, which can be due to the particle aggregation that might add some extra space between alginate chains (free volume) and make the structure more vulnerable to the heat. These results corroborate the conclusions made based on the *DP* values determined by IGC.

The results of the viscoelastic curves (Figure 7) at room temperature (20 °C) show higher values of the storage modulus for the ultrasonicated and oxidized samples (Figure 7A, curves c-e) compared to samples prepared without ultrasonication and oxidation (Figure 7A, curve b). This indicates that the both, ultrasonication and oxidation improve the stiffness of the polymer. In the temperature range of 0–70 °C, E' values decrease, which can be attributed to the increase of the molecular mobility of the polymer chains (less external force is required for deformation). Above 70 °C, the E' values of the polymers start to increase again until the complete degradation of samples occurs (at approx. 200 °C). The improvement in E' for 10 % US TOCNCs/SA can be explained by the formation of a 3D network of interconnecting layers in the polymer matrix, which is formed by the strong intermolecular hydrogen bonding between nanocrystals and the alginate (Kumar et al., 2017). The 10% US TOCNCs/SA nanocomposite exhibits the highest value of E' among all tested film samples (4.499 GPa; Table 3), while the pure alginate film displayed the lowest value of E'. This is due to the very soft and brittle nature of the alginate. The results indicate that the orientation of carboxylate CNCs in the alginate matrix is homogenized by ultrasonication, which leads to the strong interfacial interaction between the reinforcing phase and the matrix phase and facilitate the uniform dispersion CNCs particles within the alginate matrix.

Loss modulus E'' represents the ability of the material to dissipate energy (as heat) which reflects the irreversible mechanical deformation of the material. In the same temperature region (0–50 °C), the highest loss modulus E'' was measured for ultra-sonicated and oxidized nanocomposites (Figure 7B, curves c-e). In pure alginate and 10% CNFs/SA, the loss modulus (E″) were lower, which suggests that these two samples are less prone to plastic deformation in the mentioned temperature region.

The ratio between the loss and storage modulus is called mechanical loss factor (tan δ). It represents internal friction and damping. The damping properties of the material give the balance between elastic and viscous phases in a polymeric structure (Figure 7C). More intensive

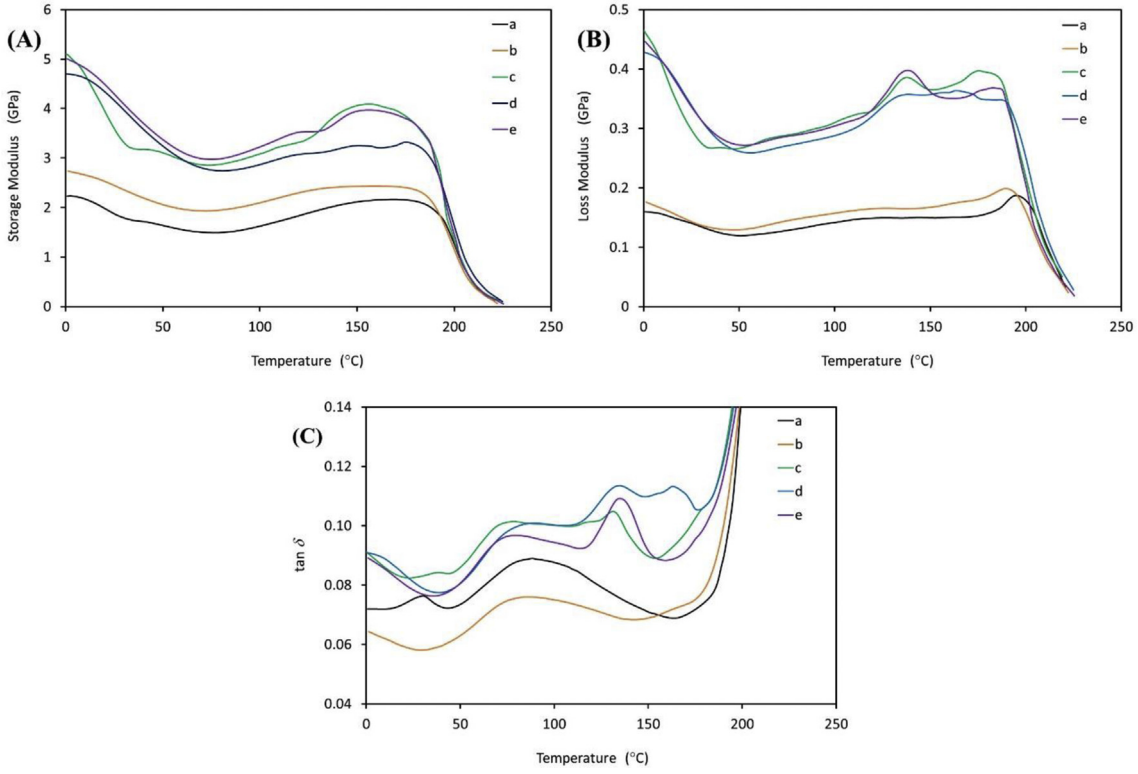

Figure 7. Graphical representations of (A) Storage modulus (E'), (B) Loss modulus (E') and (C) Damping Coefficient (tan δ) *versus* temperature. Curves are for SA film (a), 10% CNFs/SA (b), 10% US CNFs/SA (c), 10% TOCNCs/SA (d) and 10% US TOCNCs/SA (e) nanocomposites.

movement of structural elements shows higher damping effect and therefore has higher loss factor values. In the first relaxation region (0–50 °C), values of tan δ are lower for pure alginate and 10% CNFs/SA samples, where the movement of structural elements and ability of damping are low. When the temperature increased above 50 °C, movement of structural elements again became more intensive in all samples and consequently values of tan δ increased. The reason is the more intensive movement of structural elements due to the increase of the viscous component in the samples exposed to heat. Values of tan δ rapidly increased for all samples near the temperature of 200 °C due to the degradation of their molecular structure.

As observed using other analytical methods, DMA results also prove the reinforcement effect of nanocellulose in the alginate matrix, especially when ultrasonicated TOCNCs were used. Moreover, 120% enhancement in the storage modulus (from 1.980 GPa to 4.499 GPa) with the introduction of 10% US TOCNCs in SA proves that the studied material is worthy in many structural and packaging applications due to its comparatively high mechanical performance.

4. Conclusions

In order to valorize kapok, two types of nanocelluloses, cellulose nanofibrils (CNFs) and cellulose nanocrystals (CNCs) obtained by TEMPO-mediated oxidation, were characterized and the properties of the resultant bio-composites studied. Also, the use of ultrasonification, as a dispersive method, was evaluated. Therefore, improved-performance bio-nanocomposites were prepared using kapok cellulose nanofibrils (before and after TEMPO-mediated oxidation) and sodium alginate, with and without ultrasonication treatment, followed by solution casting method. AFM, ^{13}C-CPMAS NMR and IGC studies indicated that the TEMPO-mediated oxidation process of CNFs promotes the disintegration of the CNFs into smaller particles, cellulose nanocrystals (TOCNCs) with carboxyl groups at the surface. Surface characterization of nanocomposite films by SEM, AFM and IGC revealed the improved dispersion of TOCNCs particles in the alginate matrix than with CNFs. These measurements also showed that the ultrasonication of TOCNCs has a significant impact in reducing the surface roughness values of the resulting nanocomposite systems and improving the mechanical strength of the polymer. The overall results confirmed the outstanding efficiency of TOCNCs as an ideal reinforcement unit in alginate biopolymer and the ultrasonification as a dispersive efficient method. Also, it was demonstrated that these bio-nanocomposites can have potential applications in several areas: their porosity and smooth character makes them suitable to be applied as a scaffold in the tissue engineering; and the comparatively high mechanical performance make them candidate for many structural and packaging applications.

Declarations

Author contribution statement

B. Deepa: Conceived and designed the experiments; Performed the experiments; Analyzed and interpreted the data; Wrote the paper.

N. Cordeiro: Analyzed and interpreted the data; Contributed reagents, materials, analysis tools or data; Wrote the paper.

M. Faria: Performed the experiments; Analyzed and interpreted the data; Wrote the paper.

E. Abraham, G. Primc, Y. Pottathara & M. Leskovšek: Analyzed and interpreted the data; Contributed reagents, materials, analysis tools or data.

M. Gorjanc & M. Mozetič: Contributed reagents, materials, analysis tools or data.

S. Thomas & L. Pothan: Conceived and designed the experiments; Analyzed and interpreted the data; Contributed reagents, materials, analysis tools or data.

Funding statement

B. Deepa gratefully acknowledges the Council of Scientific and Industrial Research (CSIR), Govt. of India, New Delhi for their financial support. N. Cordeiro would like to thank the National program for Scientific Equipment Renewal, POCI 2010, for sponsoring IGC work (FEDER and Foundation for Science and Technology). M. Leskovšek and M. Gorjanc acknowledge Slovenian Research Agency for their financial support (research core funding P2-0213 and P2-0082). B. Deepa would also like to thank Dr. Daniel Pasquini, Institute of Chemistry, Federal University of Uberlândia, Brazil, for carrying out the AFM analysis of nanocellulose samples.

Competing interest statement

The authors declare no conflict of interest.

Additional information

No additional information is available for this paper.

References

Abdollahi, M., Alboofetileh, M., Rezaei, M., Behrooz, R., 2013. Comparing physico-mechanical and thermal properties of alginate nanocomposite films reinforced with organic and/or inorganic nanofillers. Food Hydrocolloids 32, 416–424.

Abraham, E., Deepa, B., Pothan, L.A., Jacob, M., Thomas, S., Cvelbar, U., Anandjiwala, R., 2011. Extraction of nanocellulose fibrils from lignocellulosic fibres: a novel approach. Carbohydr. Polym. 86, 1468–1475.

Chaichi, M., Hashemi, M., Badii, F., Mohammadi, A., 2017. Preparation and characterization of a novel bionanocomposite edible film based on pectin and crystalline nanocellulose. Carbohydr. Polym. 157, 167–175.

Cheng, F., Liu, C., Wei, X., Yan, T., Li, H., He, J., Huang, Y., 2017. Preparation and characterization of 2, 2, 6, 6-Tetramethylpiperidine-1-oxyl (TEMPO)-oxidized cellulose nanocrystal/alginate biodegradable composite dressing for hemostasis applications. ACS Sustain. Chem. Eng. 5, 3819–3828.

Cordeiro, N., Gouveia, C., Moraes, A.G.O., Amico, S.C., 2011. Natural fibres characterization by inverse gas chromatography. Carbohydr. Polym. 84, 110–117.

Deepa, B., Abraham, E., Cherian, B.M., Bismarck, A., Blaker, J.J., Pothan, L.A., Kottaisamy, M., 2011. Structure, morphology and thermal characteristics of banana nano fibres obtained by steam explosion. Bioresour. Technol. 102, 1988–1997.

Deepa, B., Abraham, E., Cordeiro, N., Mozetic, M., Mathew, A.P., Oksman, K., Pothan, L.A., 2015. Utilization of various lignocellulosic biomass for the production of nanocellulose: a comparative study. Cellulose 22, 1075–1090.

Deepa, B., Abraham, E., Pothan, L.A., Cordeiro, N., Faria, M., Thomas, S., 2016. Biodegradable nanocomposite films based on sodium alginate and cellulose nanofibrils. Materials 9 (50), 1–11.

Habibi, Y., Chanzy, H., Vignon, M.R., 2006. TEMPO-mediated surface oxidation of cellulose whiskers. Cellulose 13, 679–687.

Hassan, E.A., Fadel, S.M., Hassan, M.L., 2018. Influence of TEMPO-oxidized NFC on the mechanical, barrier properties and nisin release of hydroxypropyl methylcellulose bioactive films. Int. J. Biol. Macromol. 113, 616–622.

Hu, Z.-H., Omera, A.M., Ouyanga, X.-K., Yu, D., 2018. Fabrication of carboxylated cellulose nanocrystal/sodium alginatehydrogel beads for adsorption of Pb(II) from aqueous solution. Int. J. Biol. Macromol. 108, 149–157.

Huq, T., Salmieri, S., Khan, A., Khan, R.A., Le Tien, C., Riedl, B., Lacroix, M., 2012. Nanocrystalline cellulose (NCC) reinforced alginate based biodegradable nanocomposite film. Carbohydr. Polym. 90, 1757–1763.

Isogai, A., Saito, T., Fukuzumi, H., 2011. TEMPO-oxidized cellulose nanofibres. Nanoscale 3, 71–85.

Kim, J.H., Parka, S., Kim, H., Kim, H.J., Yang, Y.-H., Kim, Y.H., Jung, S.-K., Kan, E., Lee, S.H., 2017. Alginate/bacterial cellulose nanocomposite beads prepared using Gluconacetobacterxylinus and their application in lipase immobilization. Carbohydr. Polym. 157, 137–145.

Kumar, A., Rao, K.M., Han, S.S., 2017. Development of sodium alginate-xanthan gum based nanocomposite scaffolds reinforced with cellulose nanocrystals and halloysite nanotubes. Polym. Test. 63, 214–225.

Lai, C., Sheng, L., Liao, S., Xi, T., Zhang, Z., 2013. Surface characterization of TEMPO-oxidized bacterial cellulose. Surf. Interface Anal. 45, 1673–1679.

Laurén, P., Somersalo, P., Pitkänen, I., Lou, Y.-R., Urtti, A., Partanen, J., Seppala, J., Madetoja, M., Laaksonen, T., Makitie, A., Yliperttula, M., 2017. Nanofibrillar cellulose-alginate hydrogel coated surgical sutures as cell-carrier systems. PLoS One 12 (8), e0183487.

Moon, R.J., Martini, A., Nairn, J., Simonsen, J., Youngblood, J., 2011. Cellulose nanomaterials review: structure, properties and nanocomposites. Chem. Soc. Rev. 40, 3941–3994.

Qin, X., Xia, W., Sinko, R., Keten, S., 2015. Tuning glass transition in polymer nanocomposites with functionalized cellulose nanocrystals through nanoconfinement. Nano Lett. 15, 6738–6744.

RoyChowdhury, P., Kumar, V., 2006. Fabrication and evaluation of porous 2,3-dialdehydecellulose membrane as a potential biodegradable tissue-engineering scaffold. J. Biomed. Mater. Res. A 76, 300–309.

Saito, T., Kimura, S., Nishiyama, Y., Isogai, A., 2007. Cellulose nanofibres prepared by TEMPO-mediated oxidation of native cellulose. Biomacromolecules 8, 2485–2491.

Saito, T., Shibata, I., Isogai, A., Suguri, N., Sumikawa, N., 2005. Distribution of carboxylate groups introduced into cotton linters by the TEMPO-mediated oxidation. Carbohydr. Polym. 61, 414–419.

Sharma, P.R., Joshi, R., Sharma, S.K., Hsiao, B.S., 2017. A simple approach to prepare carboxycellulose nanofibres from untreated biomass. Biomacromolecules 18, 2333–2342.

Shen, X.-J., Huang, P.-L., Chen, J.-H., Wu, Y.-Y., Liu, Q.-Y., Sun, R.-C., 2017. Comparison of acid-hydrolyzed and TEMPO-oxidized nanocellulose for reinforcing alginate fibers. BioResources 12 (4), 8180–8198.

Sirviö, J.A., Kolehmainen, A., Liimatainen, H., Niinimäki, J., Hormi, O.E.O., 2014. Biocomposite cellulose-alginate films: promising packaging materials. Food Chem. 151, 343–351.

Viëtor, R.J., Newman, R.H., Ha, M.A., Apperley, D.C., Jarvis, M.C., 2002. Conformational features of crystal-surface cellulose from higher plants. Plant J. 30, 721–731.

Yasir Beeran, P.T., Bobnar, V., Gorgieva, S., Grohens, Y., Finšgar, M., Thomas, S., Kokol, V., 2016. Mechanically strong, flexible and thermally stable graphene oxide/nanocellulosic films with enhanced dielectric properties. RSC Adv. 6, 49138–49149.

Zhou, Y., Saito, T., Bergström, L., Isogai, A., 2018. Acid-free preparation of cellulose nanocrystals by TEMPO oxidation and subsequent cavitation. Biomacromolecules 19, 633–639.